Dendritic mechanisms underlying the coupling of the dendritic with the axonal action potential initiation zone of adult rat layer 5 pyramidal neurons

M. E. Larkum, J. J. Zhu and B. Sakmann

Abteilung Zellphysiologie, Max-Planck-Institut für medizinische Forschung, Jahnstraße 29, D-69120 Heidelberg, Germany

(Received 24 October 2000; accepted after revision 16 January 2001)

1. Double, triple and quadruple whole-cell voltage recordings were made simultaneously from different parts of the apical dendritic arbor and the soma of adult layer 5 (L5) pyramidal neurons. We investigated the membrane mechanisms that support the conduction of dendritic action potentials (APs) between the dendritic and axonal AP initiation zones and their influence on the subsequent AP pattern.

2. The duration of the current injection to the distal dendritic initiation zone controlled the degree of coupling with the axonal initiation zone and the AP pattern.

3. Two components of the distally evoked regenerative potential were pharmacologically distinguished: a rapidly rising peak potential that was TTX sensitive and a slowly rising plateau-like potential that was Cd^{2+} and Ni^{2+} sensitive and present only with longer-duration current injection.

4. The amplitude of the faster forward-propagating Na^+-dependent component and the amplitude of the back-propagating AP fell into two classes (more distinctly in the forward-propagating case). Current injection into the dendrite altered propagation in both directions.

5. Somatic current injections that elicited single Na^+ APs evoked bursts of Na^+ APs when current was injected simultaneously into the proximal apical dendrite. The mechanism did not depend on dendritic Na^+–Ca^{2+} APs.

6. A three-compartment model of a L5 pyramidal neuron is proposed. It comprises the distal dendritic and axonal AP initiation zones and the proximal apical dendrite. Each compartment contributes to the initiation and to the pattern of AP discharge in a distinct manner. Input to the three main dendritic arbors (tuft dendrites, apical oblique dendrites and basal dendrites) has a dominant influence on only one of these compartments. Thus, the AP pattern of L5 pyramids reflects the laminar distribution of synaptic activity in a cortical column.

One of the most striking characteristics of the cortex is the abundance of pyramidal neurons. They are always orientated with their somata in a lower layer and their apical dendrites extending exactly at right angles to the layering of the cortex, ending in a tuft usually in layers 1 and 2. There have been many suggestions as to why this architecture prevails. With the advent of visual dendritic recording techniques (Stuart *et al.* 1993; Denk *et al.* 1994), it has now become possible to probe the structure–function relationship of cortical pyramidal neurons using electrophysiological methods.

It is now well established that pyramidal neurons have a non-homogeneous distribution of voltage-gated ion channels over their somato-dendritic membrane (Johnston *et al.* 1996). These can give rise to a complex interaction of regenerative potentials that can be initiated in various sites in the neuron and then spread to other parts. In layer 5 (L5) pyramidal neurons, sodium action potentials (Na^+ APs) are initiated in the axon and propagate actively back into the dendritic tree (Stuart & Sakmann, 1994; Stuart *et al.* 1997; Buzsáki & Kandel, 1998). In addition, sodium–calcium action potentials (Na^+–Ca^{2+} APs) can be initiated in the distal apical dendrites (Reuveni *et al.* 1993; Schiller *et al.* 1997; Helmchen *et al.* 1999; Zhu, 2000). A detailed analysis of their propagation towards the soma (forward propagation) has not yet been made. Under some circumstances Na^+–Ca^{2+} APs can be isolated in the dendrites and under others they can spread to the soma and cause a burst of axonal Na^+ APs (Schiller *et al.* 1997; Schwindt & Crill, 1997; Larkum *et al.* 1999*b*). It is also clear that under some circumstances Na^+ APs can be initiated in the apical dendrite (Schwindt & Crill, 1997; Stuart *et al.* 1997; Golding & Spruston, 1998), and that

bursts of Na^+ APs can lead to the initiation of dendritic Na^+–Ca^{2+} APs (Buzsáki *et al.* 1996; Larkum *et al.* 1999*a*).

The presence of a zone in the apical dendrites for the initiation of regenerative potentials has led to the suggestion that the pyramidal neuron has two functional compartments (Spencer & Kandel, 1960; Yuste *et al.* 1994; Pinsky & Rinzel, 1994; Mainen & Sejnowski, 1996). It may be necessary to extend this notion to more than two compartments by including other regions that are capable of initiating regenerative activity such as the proximal apical dendrite or basal dendrites (Mel, 1993; Schwindt & Crill, 1997; Schiller *et al.* 2000). Several studies have shown that distal dendritic current injection leads to bursting behaviour (Pockberger, 1991; Wong & Stewart, 1992; Larkum *et al.* 1999*b*; Schwindt & Crill, 1999; Williams & Stuart, 1999; Zhu & Connors, 1999) due to the activation of voltage-dependent Ca^{2+} channels (VDCCs) and their interaction with back-propagating Na^+ APs. Thus synaptic input arriving at distal dendritic locations leads to a different pattern of APs than synaptic input to more proximal regions.

Despite their ubiquity and the obvious importance of pyramidal neurons in cortical networks, their behaviour in response to a given stimulus or combinations of stimuli is difficult to predict. Here we present an analysis of the propagation of regenerative potentials in both the forward and backward directions along the apical dendrite and the subsequent AP pattern of the neuron.

METHODS

Animal preparation

Experiments were performed in somatosensory neocortical slices from 4- to 8-week-old (120–280 g) Wistar rats. Animals were anaesthetized with halothane and decapitated according to the animal welfare guidelines of the Max-Planck Society. The brain was quickly removed and placed into cold (0–4 °C), oxygenated physiological solution containing (mM): NaCl 125, KCl 2.5, NaH_2PO_4 1.25, $NaHCO_3$ 25, $MgCl_2$ 1, dextrose 25 and $CaCl_2$ 2, at pH 7.4. Sagittal slices, 300 μm thick, were cut from the tissue blocks with a microslicer and then transferred to an oxygenated physiological solution and kept at 37.0 °C. Recordings were made from slices submerged in a chamber and stabilized using a fine nylon net attached to a platinum ring. The chamber was perfused with warmed and oxygenated physiological solution. The temperature of the bath solution in the chamber was kept at 32–35 °C. All drugs were bath applied.

Physiology

Simultaneous dual, triple, quadruple and sequential multiple recordings were performed on single, identified L5 pyramidal neurons using infrared illumination combined with differential interference contrast optics (Stuart *et al.* 1993). Somatic (5–10 MΩ) and dendritic (10–25 MΩ) recording pipettes were filled with standard intracellular solution containing (mM): potassium gluconate 105, Hepes 10, $MgCl_2$ 2, MgATP 4, sodium phosphocreatine 10, GTP 0.3 and KCl 30, with 2 mg ml^{-1} biocytin, at pH 7.3. Whole-cell recordings were made with up to four Axoclamp-2B amplifiers (Axon Instruments, Foster City, CA, USA).

Histology

After recordings, slices were fixed by immersion in 4% paraformaldehyde in 0.1 M phosphate buffer. Tissue sections were

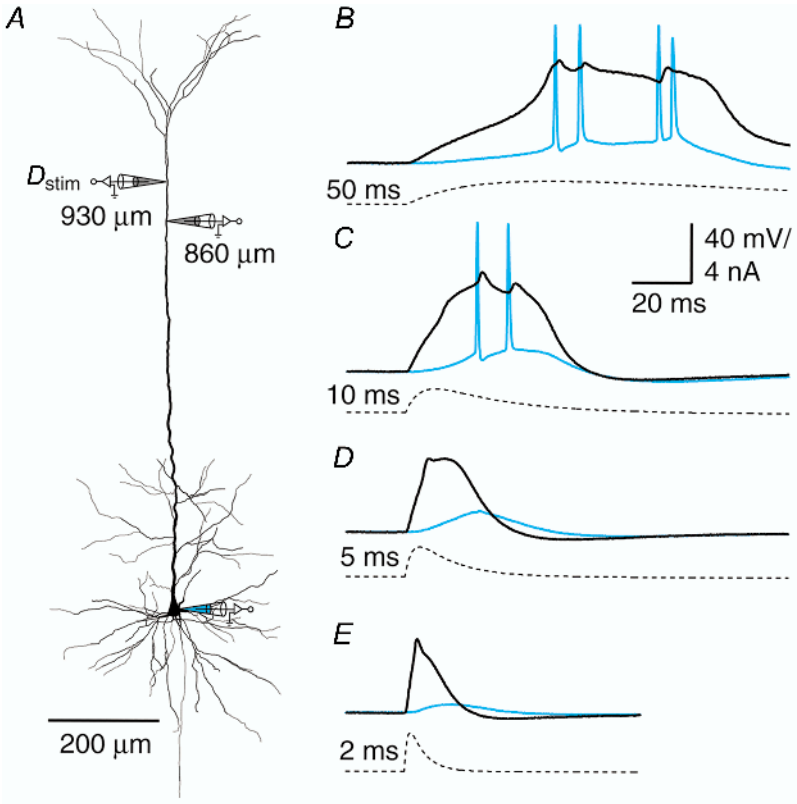

Figure 1. The effect of input time course on initiation zone coupling

A, reconstruction of biocytin-filled L5 pyramidal neuron showing the sites of current injection (D_{stim}, 930 μm from soma) and recording (860 μm from soma and at the soma). *B–E*, current injections (double exponential functions, $f(t) = (1 - e^{-t/\tau_1})e^{-t/\tau_2}$, where $\tau_2 = 4\tau_1$) for which the times to peak were set to 50, 10, 5 and 2 ms, respectively (dashed traces). The different duration current injections elicited variable-length sodium–calcium action potentials (Na^+–Ca^{2+} APs) at the dendritic recording electrode (black traces) and a variable number and pattern of sodium action potentials (Na^+ APs) at the soma (blue traces).

processed with the avidin–biotin–peroxidase method to reveal cell morphology. The dendritic morphology was reconstructed with the aid of a computerized reconstruction system (Neurolucida).

RESULTS

Relationship between dendritic Na^+–Ca^{2+} APs and axonal Na^+ APs

The effect of a dendritic Na^+–Ca^{2+} AP on the depolarization at the soma is variable between cells (Schiller *et al.* 1997; Larkum *et al.* 1999*b*; Zhu, 2000). This could be due to variability in the propagation of signals towards the soma from cell to cell, or variability in the dendritic depolarization itself. We first examined the generation of Na^+–Ca^{2+} APs in the distal dendritic initiation zone using physiologically shaped current injection.

Different EPSP-like depolarizations were generated by injecting EPSC-shaped current with different times to peak. Current injections were made via a distal pipette and recorded with another pipette also in the Na^+–Ca^{2+} AP initiation zone (Fig. 1*A*). The different input signals evoked dendritic Na^+–Ca^{2+} APs of varying duration, which in turn affected the initiation of axonal APs. Longer EPSP current injections (> 50 ms time to peak) always evoked a burst of APs at the soma and a long sodium–calcium action potential complex

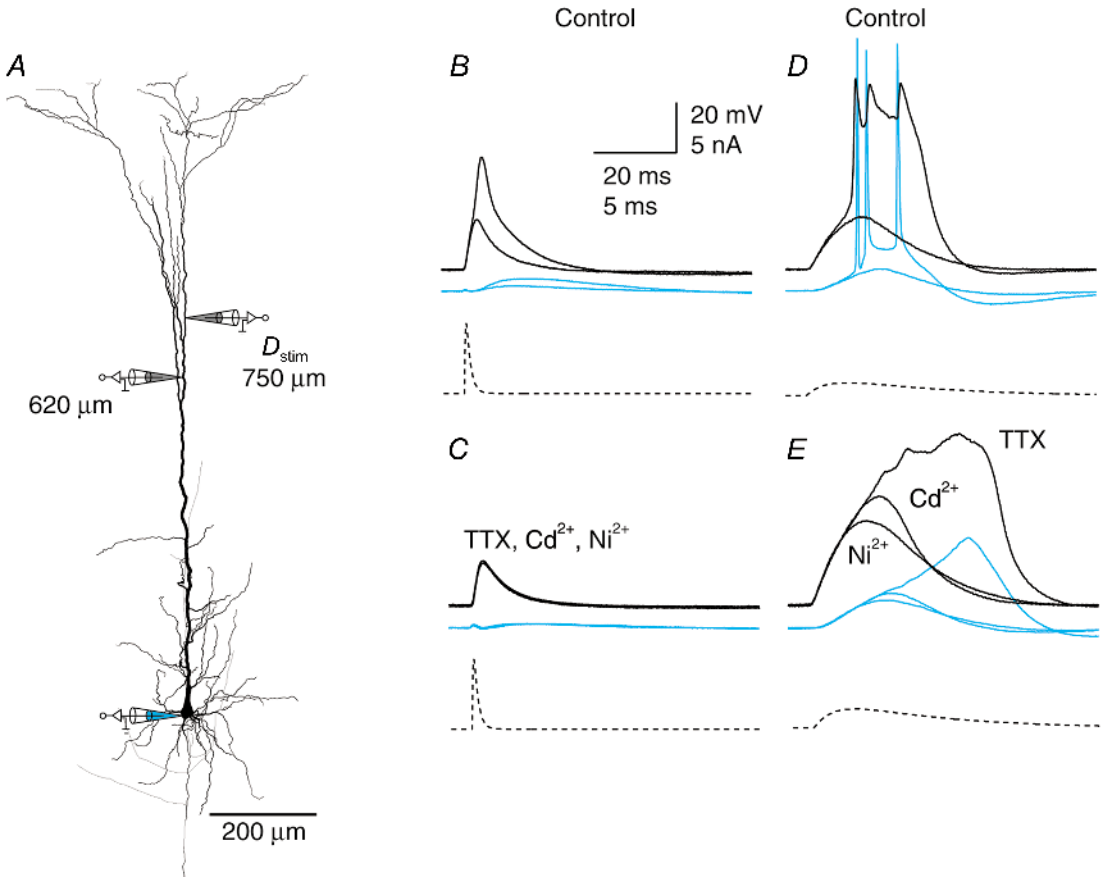

Figure 2. Na^+ and Ca^{2+} components of the dendritic potential

A, reconstruction of biocytin-filled L5 pyramidal neuron showing the sites of current injection (D_{stim}, 750 μm from soma) and recording (620 μm from soma and at the soma). *B*, short current injections (time to peak, 1 ms; dashed trace) elicited an all-or-none event, which was short and resembled a dendritic Na^+ AP (black traces) that did not propagate to the soma (blue traces) but appeared as a 'boosted EPSP'. Here traces just before and after threshold current injection are shown superimposed. *C*, application of TTX (1 μM) abolished the event and subsequent addition of Ni^{2+} and Cd^{2+} (100 and 50 μM, respectively) had no further effect. *D*, longer current injection (time to peak, 10 ms; dashed trace) elicited a complex dendritic potential with three Na^+ APs with the first peak in the dendrite (black traces) preceding the first back-propagating Na^+ AP (blue traces), but subsequent dendritic peaks following the somatic potentials. *E*, application of TTX blocked the fast rising component, the back-propagating Na^+ APs and the dendritic peaks, leaving only a long potential that could be almost completely blocked by subsequent addition of Cd^{2+} and then further blocked by Ni^{2+}.

(Na^+–Ca^{2+} AP complex) in the distal dendrite ($n = 10$). The site of the initial event with these long pulses was variable. In about half of the experiments, the dendritic regenerative activity preceded the first back-propagating AP (as in Fig. 1*B*), whereas in the other cases, the first back-propagating AP preceded the dendritic Na^+–Ca^{2+} AP complex. Shorter current injections (< 50 ms) produced regenerative responses in the dendrite with fewer or no somatic Na^+ APs (Fig. 1*C–E*). More peak current was needed to generate a dendritic Na^+–Ca^{2+} AP with shorter current injections than with longer current injections. Thus the duration of the distal current injection appears to affect both the coupling of the initiation zones and the subsequent number of back-propagating APs. This in turn affects the length of the regenerative response in the dendritic initiation zone.

The dominant ion conductance in the dendritic initiation zone was similarly dependent on the duration of the dendritic current injection. During short current injections, in which a short response was elicited in the dendrite with no back-propagating Na^+ APs, the response was blocked by the addition of 1 μM TTX, with no further block by either 50 μM Cd^{2+} or 100 μM Ni^{2+} ($n = 4$; Fig. 2*A–C*). In contrast, during longer current injections, TTX blocked only the initial steep rise in the dendritic potential and the subsequent back-propagating Na^+ APs but left a long plateau-like potential that was mostly blocked by Cd^{2+} and then completely by Ni^{2+} and Cd^{2+} together ($n = 4$; Fig. 2*D* and *E*).

Forward propagation of dendritic Na^+–Ca^{2+} APs

We examined the propagation of this initial Na^+-dependent phase of the Na^+–Ca^{2+} AP towards the soma using simultaneous triple recordings (Fig. 3*A*). The distally located pipette was used to initiate a Na^+–Ca^{2+} AP (in most cases using an EPSP waveform with a time to peak of 3.2 ms, which was an intermediate time course). A second pipette recorded the peak voltage of the forward-propagating component of the Na^+–Ca^{2+} AP at some middle location between the distally located pipette and the soma. A third electrode was placed at the soma and measured both the size of the forward-propagating component at the soma and the time of the first back-propagating Na^+ AP. The ensemble of cells investigated could be separated into two groups according to the amplitude of the forward-propagating component measured at the middle electrode. The peak amplitude either increased towards the soma to approximately the same amplitude as the somatic Na^+ AP or else it decreased to a small fraction of its initial value (Fig. 3*B*).

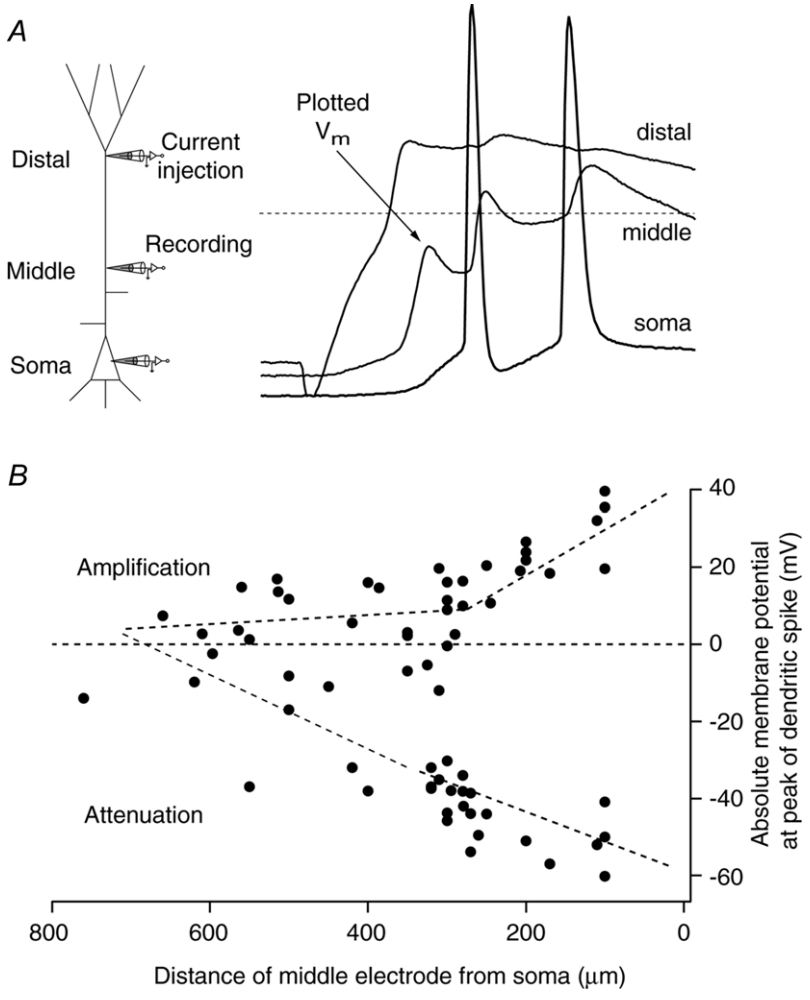

Figure 3. Forward propagation of the dendritic potential

A, schematic representation of triple recordings (left) in which a dendritic potential was generated with the distally located electrode by injection of current (time to peak, 2–5 ms). The middle electrode was used to determine the maximum depolarization of the first peak and the somatic recording to show the time of the first back-propagating Na^+ AP to check that the potential recorded at the middle electrode was propagating forwards. Dashed line represents 0 mV. *B*, the absolute membrane potential (V_m) at the peak of 67 dendritically recorded potentials from 40 neurons travelling towards the soma plotted as function of the distance of the middle electrode from the soma. The distal site varied from 560 to 860 μm from the soma (666 ± 67 μm). Dashed lines were fitted by eye through the two putative classes of forward propagation (labelled Amplification and Attenuation).

The wavefront of the forward-propagating potential in cells where it increased towards the soma often had two components. This could be shown by using multiple recordings along the apical dendrite (Fig. 4*A*). For the neuron shown in Fig. 4 the two components were clearly separated (two and three asterisks, Fig. 4*B* and *C*). Usually, however, the second component followed the first component so closely that they were nearly indistinguishable. For those cells in which the two components were separated, the first component was clearly initiated in the distal initiation zone and the second component had a much faster rising edge in the proximal dendritic trunk region. This suggests that the second component depends on the properties of the proximal apical dendritic zone and this might be a form of Na^+ AP initiation in the apical dendrite which also amplifies the forward-propagating regenerative potential.

Timing of proximal input

One way to demonstrate the active properties of the proximal trunk was to record from the proximal apical dendrite directly (200–400 μm from the soma) and alter the local membrane potential by current injection (Fig. 5*A*). In those neurons where the forward-propagating dendritic Na^+–Ca^{2+} AP failed to invade the soma, a small depolarizing current injection of 50 ms duration that preceded the Na^+–Ca^{2+} AP by 30 ms was sufficient for the forward-propagating potential to propagate well up to the soma. This in turn led to a back-propagating axonal Na^+ AP, which interacted with the

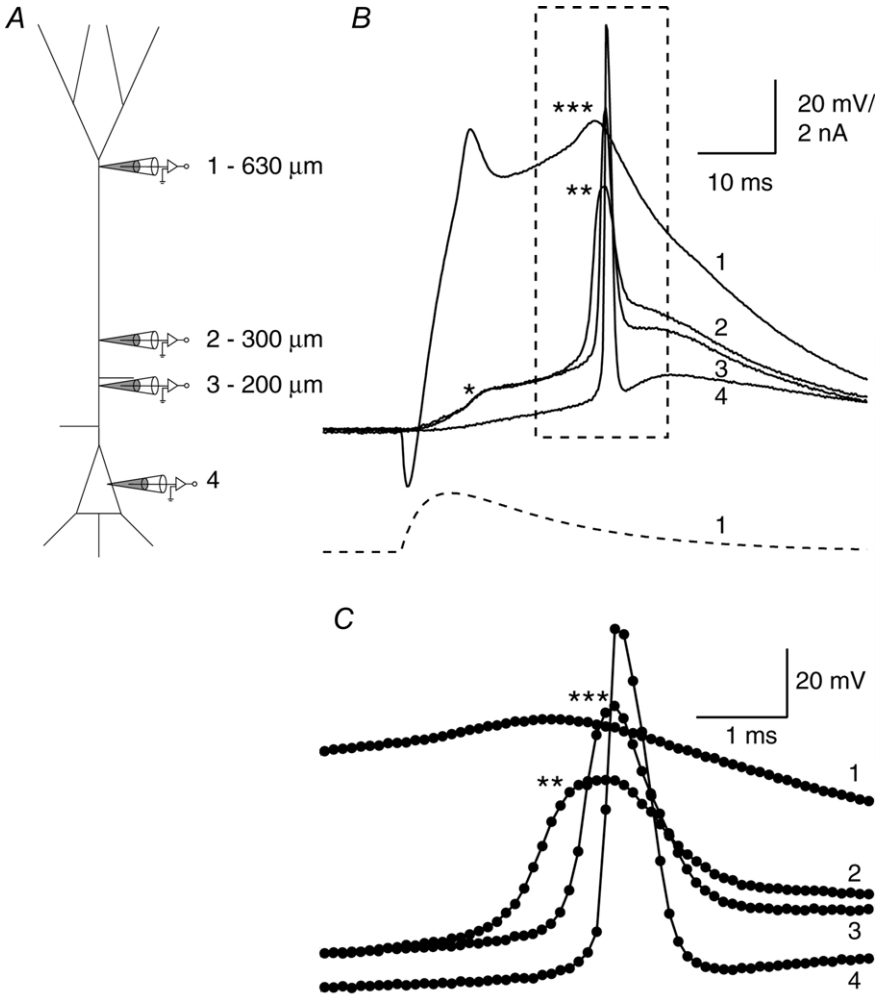

Figure 4. Two components of the forward-propagating potential

A, schematic diagram showing the electrode placement at 630 μm (1), 300 μm (2), 200 μm (3) and the soma (4) on a L5 pyramidal cell. The recording was made in two stages (first electrodes 1, 2 and 4 and then electrodes 1, 3 and 4; i.e. electrode 2 was moved to the position of electrode 3). *B*, injection of an EPSP-shaped current (bottom trace) was used to elicit a Na^+–Ca^{2+} AP in the distal dendrite. The initial component failed to propagate forwards as recorded at electrodes 2 and 3 (*****; 300 and 200 μm from the soma), but there was a second propagating component, also starting at the most distal electrode, that decreased in amplitude up to 300 μm (******) and later increased to 200 μm(*******) before reaching full height at the soma. *C*, the boxed region from *B* on an enlarged time scale showing the sequence of events.

dendritic regenerative response to ensure a longer-lasting regenerative dendritic Ca^{2+} potential, which in turn led to a burst (Fig. 5*B*). Alternatively, the somatic invasion by a forward-propagating dendritic Na^{+}–Ca^{2+} AP could be blocked by a hyperpolarizing pulse of similar timing and duration (Fig. 5*C*).

The effect of changing the membrane potential in the proximal apical dendrite was most pronounced when the forward-propagating event was evoked during injection of the current pulse into the proximal apical dendrite (Fig. 6*A*–*C*). In Fig. 6, the forward-propagating potential was most affected by a change in membrane potential (V_m) during the proximal injection but forward propagation was also influenced 5 ms after the proximal current injection at higher intensities (Fig. 6*D*). After 35 ms, the preceding V_m change in the proximal dendrite had no influence on propagation (Fig. 6*D*). As shown in Fig. 3, the propagation of the distally evoked regenerative potential was variable between different cells under control conditions. However, its propagation

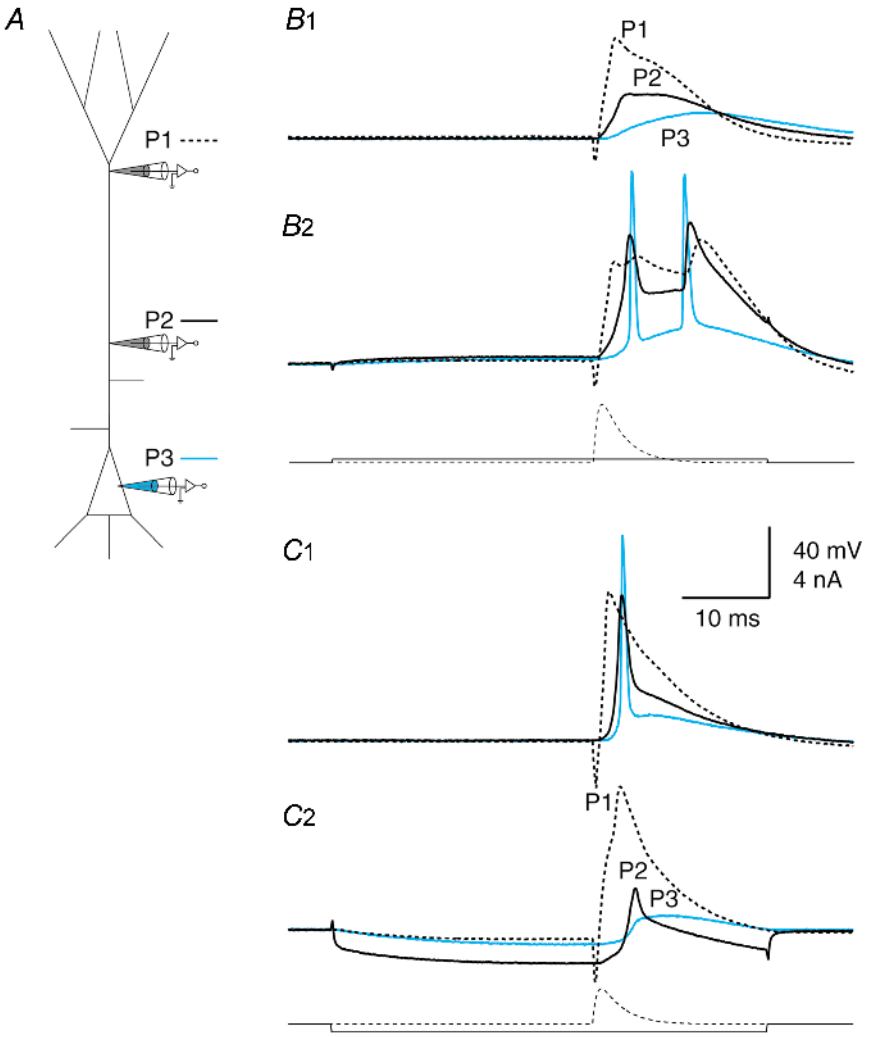

Figure 5. Modulating the amplitude of the forward-propagating potential

A, schematic diagram showing the electrode placement on a L5 pyramidal cell: distally, proximally and at the soma (P1, P2 and P3, respectively). *B*, isolated dendritic potential that was converted to a propagating potential. *B*1, current injected at the distal dendritic electrode (P1) caused a Na^{+}–Ca^{2+} AP in the distal dendrite that failed to propagate fully to the soma. *B*2, a very small current injection (200 pA pulse for 50 ms; onset 30 ms before EPSP waveform current injection at distal electrode) at the proximal electrode (300 μm from soma) caused the forward-propagating event to propagate well, leading to Na^{+} APs at the soma and a dendritic Na^{+}–Ca^{2+} AP complex. *C*, AP propagating well that was converted to an isolated dendritic potential. *C*1, an example of a cell with well-propagating forward potentials under control conditions. *C*2, hyperpolarizing current (−450 pA) injected at the proximal electrode (P2; 300 μm from the soma) caused the forward-propagating potential to fail. Current injection waveforms are shown beneath the recorded potentials.

could always be manipulated using 50 ms pulses at a proximally located dendritic pipette (middle pipette, 200–400 μm from the soma). When the proximal current injection needed just before the fast transition into good forward propagation was normalized to zero, the abrupt transition between forward propagation and failure to propagate could be averaged across different neurons (Fig. 6*E*; $n = 7$).

The forward-propagating dendritic Na^+–Ca^{2+} AP could also be blocked in some cases ($n = 8$) by injecting suprathreshold current pulses at the distal dendritic initiation site (Fig. 7). In such cases, the two-component forward-propagating potential failed at exactly the point in the rising phase where there had been a point of inflection (Fig. 7*C* and *D*, arrows), suggesting that this phase of the potential is critical for successful forward propagation past the proximal zone. Pulses were normally given at 3 s intervals, but increasing the interval to 10 s did not change the result, nor did the use of

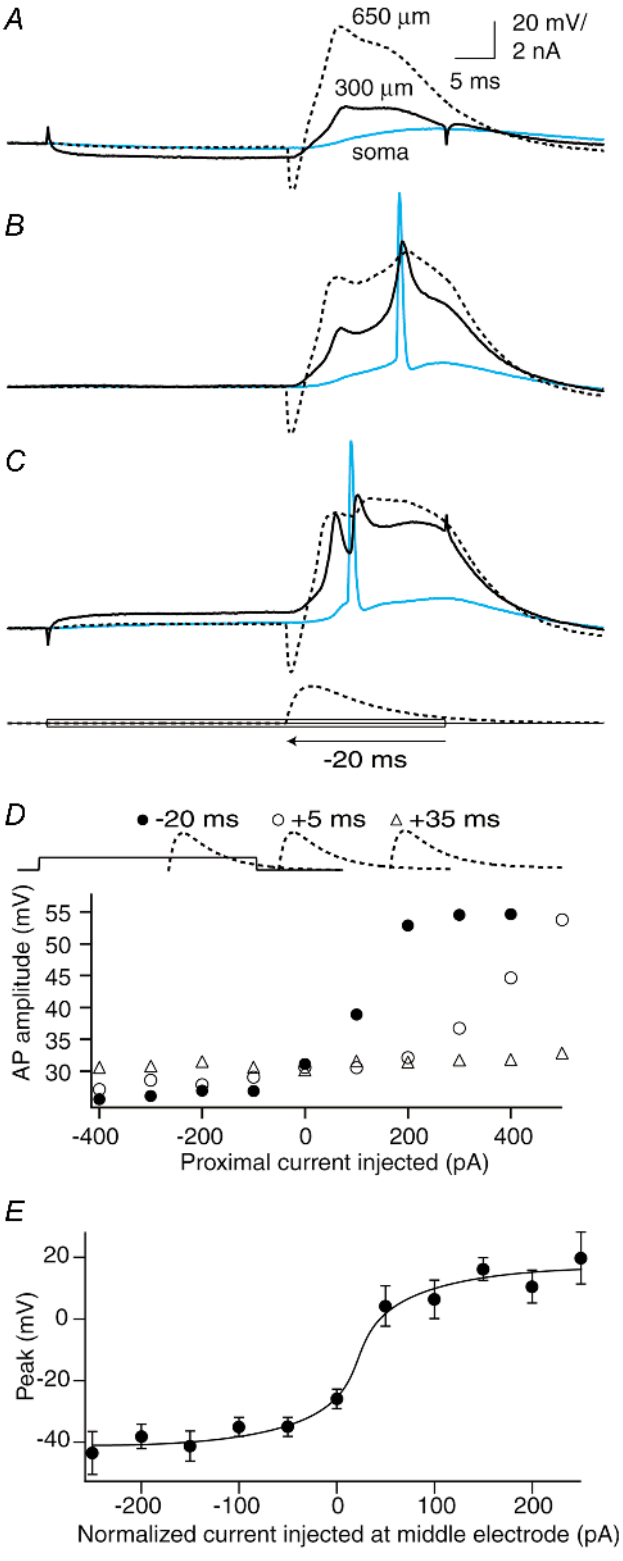

Figure 6. Timing of the input to the proximal region

A, current injected at the proximal electrode (300 μm) caused the forward-propagating dendritic Na^+–Ca^{2+} AP evoked by an EPSP-shaped waveform at the distal electrode (650 μm) to fail completely towards the soma. *B*, in this same cell the forward-propagating Na^+–Ca^{2+} AP was in an intermediate state of propagation under control conditions and showed two components. The second rising component was interrupted by the presence of a back-propagating Na^+ AP from the soma. *C*, depolarizing current at the proximal electrode caused the forward propagation to be completely active and only one component was then apparent. Further current injection led to more Na^+ APs. *D*, the onset of an EPSP-shaped waveform injected at the distal electrode was moved relative to the end of the 50 ms step pulse injection at the proximal dendritic electrode. Here, we show data from 20 ms before the end of the proximal injection (●), and 5 ms (○) and 35 ms (△) after the end of the proximal injection (shown above the graph schematically). The least current required to improve propagation of the dendritic Na^+–Ca^{2+} AP was needed when it was injected during the proximal current injection (●). *E*, the sharp cutoff between APs that propagated well and those that propagated badly for a number of cells ($n = 7$) is shown by aligning the last point still under the half-amplitude point to 0 pA. The actual current injected for this point varied from −500 to +400 pA (mean, 100 ± 290 pA) depending on the initial conditions of coupling for the cell. The shift between good propagation and failure to propagate occurred within ~50 pA.

decreasing current steps instead of increasing current steps. In other cells where the generation of a somatic AP did not change as a result of increasing current injections, there was still a decrease in the size of the forward-propagating peak with further current injection ($n = 4$; data not shown). The exact mechanism is likely to depend on the combination of Na^+ and K^+ conductances whose activation and inactivation depend on the time taken from the beginning of the current injection to the initiation of the dendritic regenerative potential (larger current injections evoked the dendritic potential earlier). Full propagation towards the soma also resulted in a slight increase at the distal site, following the second phase increase in the proximal dendrite but preceding the back-propagating Na^+ AP from the soma. This suggests that the additional component arises in the proximal apical dendrite and propagates in both directions (towards the soma and back into the apical tuft).

Backward propagation of Na^+ APs

Back-propagating APs have been shown to attenuate in amplitude as a function of distance along the apical dendrite with inactivation of Na^+ channels leading to decreasing amplitudes during a train (Spruston *et al.* 1995; Stuart *et al.* 1997). A closer examination of this phenomenon with multiple dendritic recordings (Fig. 8*A*) revealed that the inactivation of Na^+ channels during a train of back-propagating APs is observed at distances greater than ~300 μm from the soma (Fig. 8*B*). Further away than ~300 μm there is a rapid onset of the inactivation over the subsequent 300–500 μm segment of the apical dendrite (Fig. 8*C*). Thus, the back propagation of the AP in the proximal apical dendrite is not affected by the previous AP pattern of the pyramidal neuron, in contrast to the back propagation of the AP in the distal apical tuft.

Unlike the amplitude of the last (Na^+-inactivated) AP during a train, that of the initial back-propagating AP varied from cell to cell with the variation between neurons increasing with distance from the soma (Fig. 8*D*; $n = 112$). This was also true of the latency of the back-propagating AP (measured by the time of half-

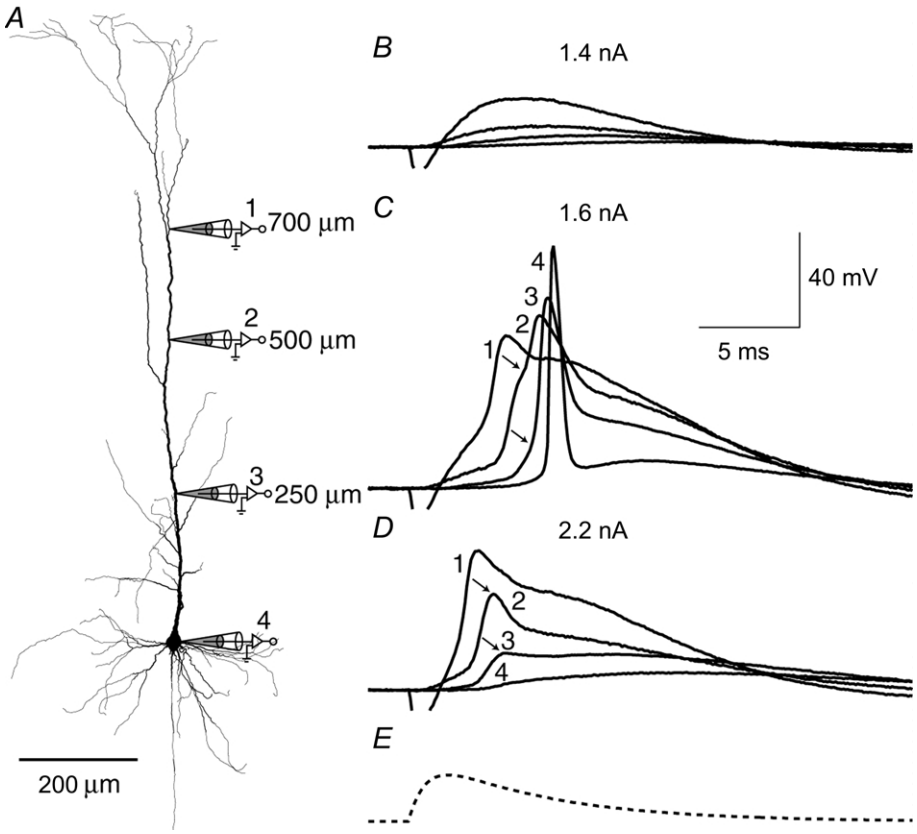

Figure 7. Critical region for forward propagation

A, reconstruction of biocytin-filled L5 pyramidal neuron showing the locations of dendritic recording. The experiment consisted of two triple recordings with the proximal electrode (250 μm) exchanged for the less proximal electrode (500 μm) but the distal (700 μm) and somatic electrodes remaining in place. *B*, an EPSP-shaped current injection at the distal electrode (shown in *E*) of 1.4 nA at the peak failed to evoke a dendritic Na^+–Ca^{2+} AP. *C*, however, at the threshold of 1.6 nA, the dendritic Na^+–Ca^{2+} AP was evoked and propagated well towards the soma. The rising phase clearly had two components at 500 μm and probably also at 250 μm (points of inflection indicated by arrows). *D*, with further current injection (2.2 nA) the potential failed at the previous turning point (marked by arrows) and rapidly decreased towards the soma, indicating the presence of a critical region in the apical dendrite that needs to be active for complete forward propagation.

amplitude). The latency of the last AP in a train was not significantly different to the latency of the first AP (Fig. 8*E*), showing that the latency is not significantly influenced by Na^+ regenerative activity. The conduction velocity, calculated by fitting a line (through zero) to the latencies of the first AP (dashed line, Fig. 8*E*), was found to be 508 μm ms^{-1}. Thus, the decrement in amplitude of the first back-propagating AP appeared to fall into two classes in a way reminiscent of the forward-propagating AP (Fig. 3*B*), which we showed above is all-or-none in its propagation towards the soma.

As with forward propagation, it was also possible to induce changes in the amplitude of back-propagating potentials with current injection in a single cell by applying negative current injection during a train of APs (Fig. 9*A* and *B*). Here, the third AP of a train (70 Hz) was substantially reduced in size at the distal site (630 μm from the soma) but not altered at the site of current injection (300 μm from the soma). This diminished AP waveform was subtracted from the control waveform to reveal a regenerative component of the back-propagating AP of approximately 40 mV in amplitude (Fig. 9*C*). This

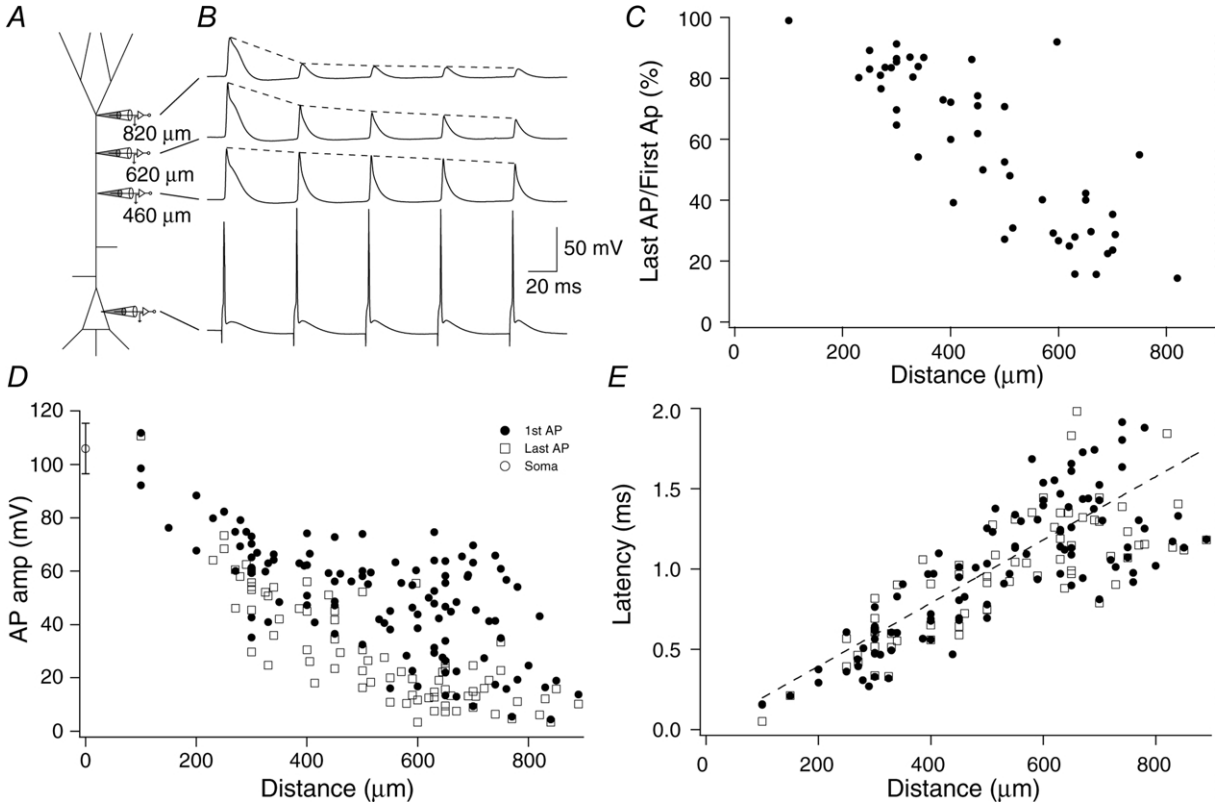

Figure 8. Attenuation of back-propagating action potentials

A, schematic diagram showing the placement of 4 electrodes on a L5 pyramidal neuron simultaneously. The 3 dendritic recordings were made at 460, 620 and 820 μm from the soma. *B*, traces corresponding to the 4 electrodes arranged vertically and sequentially. Current pulses of 2 ms in duration were injected at the somatic electrode to elicit APs at 20 Hz. The first back-propagating Na^+ AP showed little reduction over the interval 460–820 μm. The last Na^+ AP, however, was significantly reduced at 820 μm relative to the initial AP but not at 460 μm with an intermediate amplitude at 620 μm. Dashed lines are superimposed to emphasize the rate of decay of the back-propagating APs. *C*, percentage amplitude of the last AP (compared to the first AP) in a train shown as a function of distance from the soma. Only cases where the first AP in the train propagated well (> 40 mV) are shown, for clarity. Here, the inactivation of the AP propagation during trains starts to occur around 300 μm and is proportionately more attenuated at distal locations. *D*, amplitudes of 112 back-propagating APs shown as a function of distance from the soma for both the first AP in a train (●) and the last AP (□). The amplitude of the first back-propagating AP becomes progressively more variable with distance. The last back-propagating AP in a train becomes progressively smaller after around 300 μm, diverging from the amplitude of the first back-propagating AP to form two classes of propagation as in the forward-propagating case. The amplitude of the somatic AP is shown (○) with standard deviation at 0 μm. *E*, the latency of the time of half-amplitude of the first dendritic back-propagating AP in a train (●) and last AP (□) after the time of half-amplitude at the soma, plotted as a function of distance. The dashed line represents a straight line fit to the first AP in each train. The slope representing the speed of propagation was 0.508 m s^{-1}.

potential could even be detected at the proximal location as a deflection on the falling phase (Fig. 9*C*, black lines) and the peak *followed* the peak of the potential at the distal site (Fig. 9*D*). In another parallel to forward propagation, two components could sometimes be discerned in the rising phase of the back-propagating potential (Fig. 9*E*).

The opposite effect on the back-propagating AP was caused by depolarization of the distal dendrite (Fig. 10*A* and *B*). In cells that generated a small initial back-propagating AP, the amplitude was increased by successively larger current injections into either the distal or the proximal region. Eventually the back-propagating AP reached a constant amplitude (Fig. 10*B* and *D*). When sufficient current was injected into the dendrite, the back-propagating AP caused an initial AP burst (Fig. 10*B*). The increase in amplitude of the initial back-propagating AP occurred over a larger range of depolarizing input current than that of the forward-propagating potential so that a series of intermediate amplitude APs was obtained (Fig. 10*D*; ●). The last AP in a train was not increased by current injection (Fig. 10*D*; ○).

Coupling of the dendritic and axonal initiation zones and AP bursting

Thus it appears that the membrane potential along the apical dendrite is critical for the propagation of APs in both directions and therefore for the *coupling* of the two

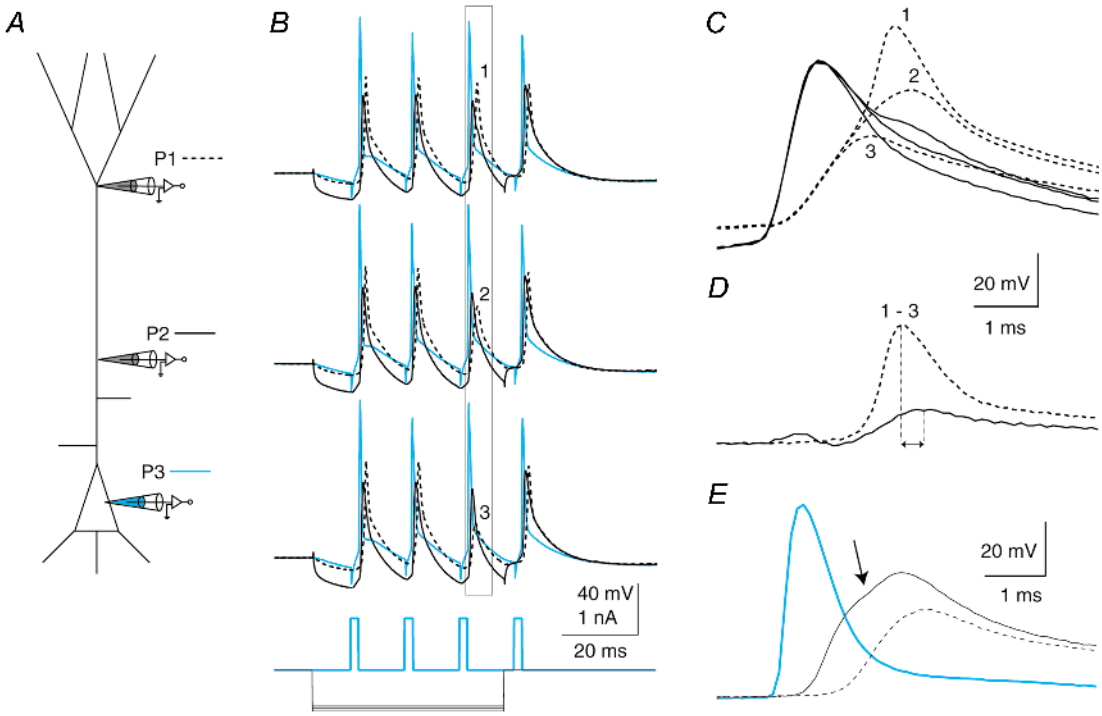

Figure 9. Two classes of back propagation

A, schematic diagram showing the placement of 3 electrodes on a L5 pyramidal neuron simultaneously. *B*, a train of back-propagating APs was elicited by current injections at the soma at 70 Hz with progressively larger hyperpolarizing current (−600 to −700 pA) injected at the proximal electrode (300 μm from the soma). (Somatic recording, P3, blue; proximal recording (300 μm), P2, black; and distal recording, 630 μm, P1, dashed line.) The hyperpolarization eventually caused the third AP in the train to decrease in amplitude, revealing the presence of a mechanism maintaining the amplitude of the back propagation of APs. *C*, expanding the time scale for the boxed region in *B* and overlaying the traces shows the two-component nature of the back-propagating AP at the distal site just before inactivation (1), during (2) and after full inactivation (3), black traces. A small depolarization is visible at the proximal site (black traces) following the peak at the proximal site. *D*, by subtracting trace 3 from trace 1, the regenerative component of the back-propagating AP is revealed to arise first at the distal location and reflected back towards the soma. Peaks are shown by vertical lines. *E*, a different cell in which the back-propagating AP clearly had two components under control conditions. Recordings were made at 170 μm (dashed trace), 420 μm (black trace) and 630 μm (blue trace) from the soma. The point of inflection revealing the existence of a further regenerative component on the recording from the 420 μm site is shown by an arrow.

AP initiation zones. To examine this further we changed the membrane potential in all compartments of the cell and measured the effect on coupling.

Increasing $[K^+]_o$ by 5 mM to 7.5 mM depolarized the neurons progressively over the course of a few minutes. Under these conditions the threshold for generating a Na^+–Ca^{2+} AP in the distal dendrite decreased and the number of Na^+ APs in the subsequent Na^+–Ca^{2+} AP complex increased (Fig. 11*B–D*). After 15 min in high K^+ solution, the cells typically started to burst spontaneously (data not shown), indicating that dendritic depolarization enhances AP bursting. The same effect was generated by depolarizing the cell with current injected at all three electrodes simultaneously, which ensured relatively homogeneous depolarization along the apical dendrite (Fig. 11*E*).

To examine the influence of dendritic depolarization on coupling and bursting in more detail, we used a pipette placed on the proximal apical dendrite to inject a 50 ms current pulse 30 ms before a single Na^+ AP was elicited at the soma. A third electrode recorded the potential in the distal tuft as usual (Fig. 12*A*). As the current was increased at the proximal site (200–400 μm from the soma), the falling phase of the back-propagating Na^+ AP became broader with a distinct shoulder (Fig. 12*B–D*). The area between the falling phases was largest at the proximal electrode, indicating that this was the site of the maximum change in V_m and thus probably the site of additional regenerative activity (area at proximal electrode was 23.0 ± 3.2 mV ms compared to 3.5 ± 3.3 mV ms at the soma and 6.0 ± 6.1 mV ms at the distal electrode; $n = 18$). Eventually, a second Na^+ AP was elicited that led to a burst and a Na^+–Ca^{2+} AP at the distal location. Importantly, when the same current as injected at the proximal location was added to the somatic current injection (without the proximal injection any more), it did not elicit the same AP bursting. This indicated that the proximal zone contributed actively to the generation of the burst rather than simply adding depolarization to the AP initiation zone.

But did the dendritic Na^+–Ca^{2+} AP cause the burst of APs or vice versa? To test this we repeated the same experiment before and after the addition of 50 μM Cd^{2+} and 100 μM Ni^{2+} to the extracellular solution (Fig. 13). Before the addition of the VDCC blockers a small

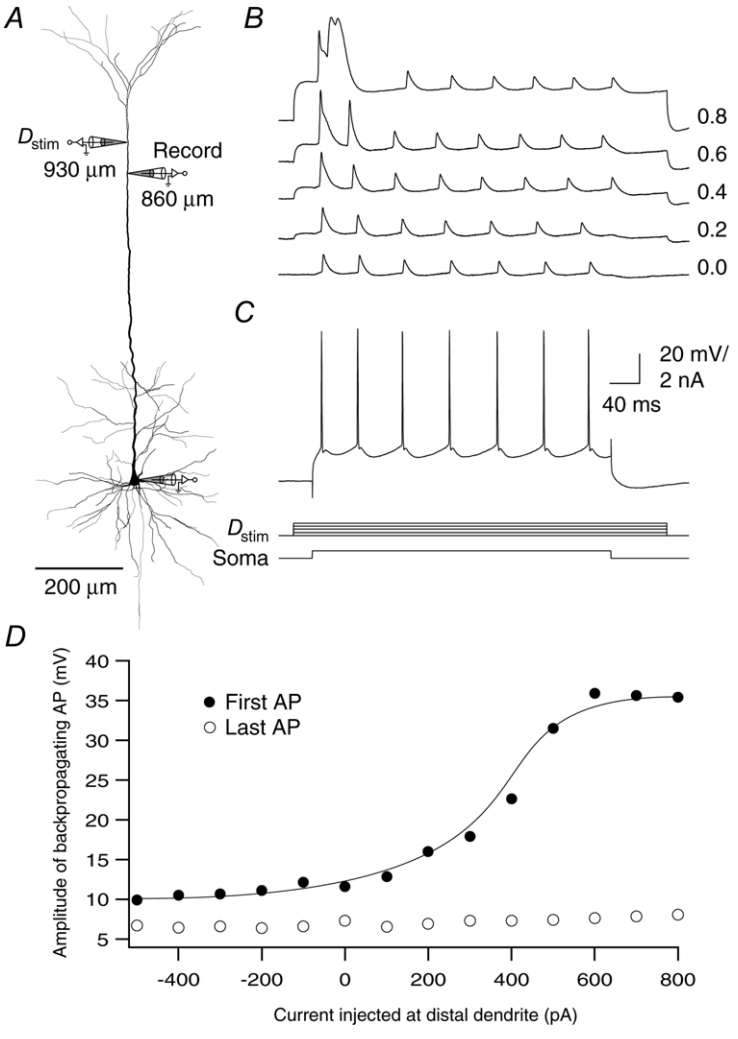

Figure 10. Dependence of back-propagating AP on dendritic V_m

A, reconstruction of a biocytin-filled L5 pyramidal neuron showing the locations of dendritic recordings. The electrode at 930 μm (D_{stim}) was used for dendritic current injection and the electrode at 860 μm for the dendritic recording. A train of back-propagating APs was generated by injecting 600 pA current for 400 ms at the soma (*C*, lower traces). *B*, a series of current injections (100 pA steps) at the dendritic location for 500 ms caused the first back-propagating AP to progressively increase in size. It eventually initiated a burst of APs at the soma followed by a calcium spike in the dendrite. *C*, the cell fired regularly when no current was injected at the dendritic site. Current injection is represented below the AP traces. *D*, the amplitude of the back-propagating AP recorded at the dendritic location is plotted as a function of the current injected at the nearby dendritic location.

injection of current at the proximal site converted to a single Na^+ AP either a doublet or a triplet of Na^+ APs (Fig. 13*B* and *C*). This was always associated with a Na^+–Ca^{2+} AP at the distal location. After the addition of the blockers, the doublet of Na^+ APs remained at the soma but the dendritic Na^+–Ca^{2+} AP and any additional APs were abolished ($n = 5$). This indicates that the proximal depolarization continued to enhance the generation of somatic doublet APs even when the distal initiation zone was inactivated. The same effect could be achieved by inactivating the distal initiation zone by hyperpolarizing current ($n = 2$) or by a small extracellularly evoked inhibitory potential ($n = 2$) that we have shown previously has a potent effect on the generation of dendritic Na^+–Ca^{2+} APs (Larkum *et al.* 1999*b*).

We examined the timing of the inputs required to cause the generation of a burst from a single Na^+ AP (Fig. 14). For this experiment we used four electrodes with two electrodes situated close to each other in the proximal region and one electrode at the soma and distal dendrite (Fig. 14*A*). Current was injected at the more distal of the two proximal electrodes, which was 250 μm from the soma. A 50 ms square-pulse current injection (0.4 nA) at $t = 10$ ms was injected at this electrode in each trace while an EPSP wave-shaped current was injected at the soma at time increments of 2 ms for each sweep (Fig. 14*B*1–4; times: *B*1, $t = 20$ ms; *B*2, $t = 22$ ms; *B*3, $t = 54$ ms; and *B*4, $t = 56$ ms). At times $t \leqslant 20$ ms (i.e. 10 ms after the onset of the proximal current injection) and $t \geqslant 56$ ms (46 ms after the onset of the proximal current injection) only a single Na^+ AP was elicited. At times in between these, a doublet was elicited at the soma (blue line). With further current injection at the proximal electrode (0.8 nA) a triplet was elicited with an extended potential at the distal electrode (not shown).

DISCUSSION

L5 pyramidal neurons of the adult rat neocortex have a dendritic and an axonal initiation zone, which elicit very different types of regenerative depolarizing potentials. We have shown that the pattern of Na^+ APs generated in the axon depends on the location and duration of depolarizing input to the dendritic arbor and the membrane potential along the apical dendrite, which controls the degree of coupling between the two initiation

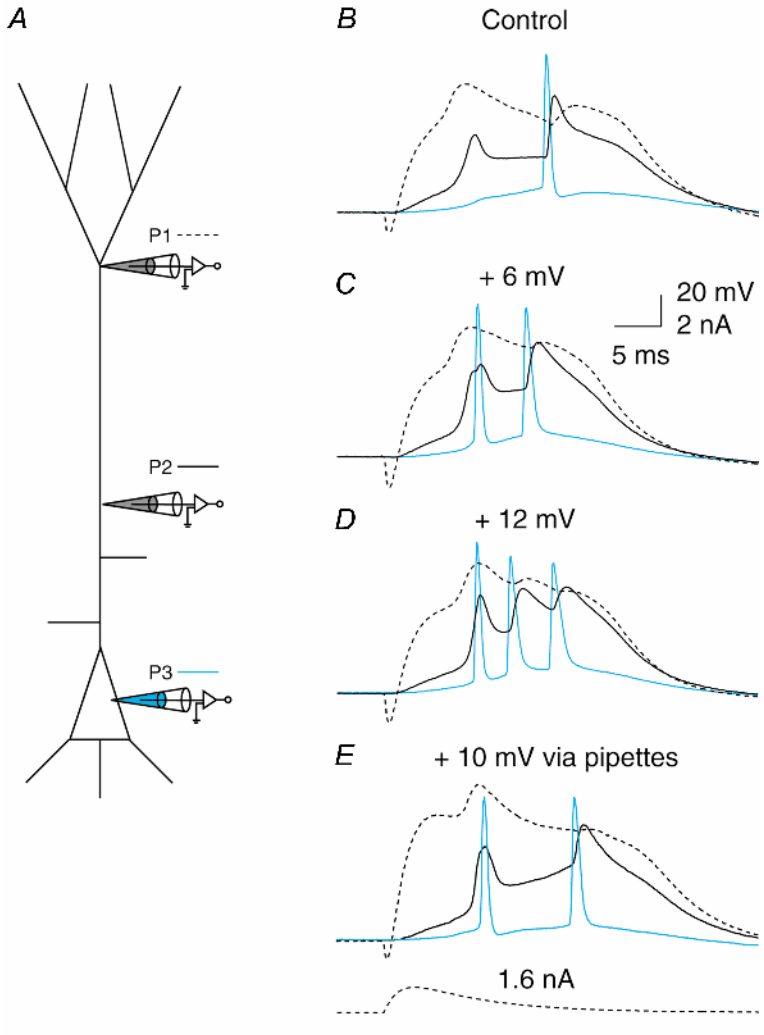

Figure 11. Depolarization enhances bursting

A, triple dendritic patch recording of a dendritic Na^+–Ca^{2+} AP initiated by injection of an EPSP-shaped waveform (1.6 nA, shown below *E*) at a distal dendritic location (P1, 650 μm from soma; dashed line) that led to a Na^+–Ca^{2+} AP and a single back-propagating AP, recorded at a more proximal location (P2, 310 μm; black line) and the soma (P3; blue line). *B*, EPSP waveform current injection at a distal dendritic location. *C*, addition of an extra 5 mM KCl to the extracellular solution (total of 7.5 mM KCl) caused progressive depolarization of the resting membrane potential. At 6 mV more depolarized than the control, the same current injection at the distal dendritic location now caused 2 APs. *D*, at 12 mV more depolarized than the control, the same current injection caused a burst of 3 APs. *E*, current injection at all three pipettes causing 10 mV depolarization had a similar effect.

zones. Thus, synaptic input arriving at different locations on the dendritic arbor is likely to exert very different influences on the pattern of APs generated by the neuron.

Forward propagation

The view of two functional compartments put forward by Yuste *et al.* (1994) can account for the types of regenerative activity that can be readily initiated in L5 neocortical pyramidal neurons *in vitro* and *in vivo* (Kim *et al.* 1995; Buzsáki *et al.* 1996; Helmchen *et al.* 1999; Larkum *et al.* 1999*b*; Zhu & Connors, 1999). The Na^+–Ca^{2+} AP initiated in the distal dendrite has two components: a fast Na^+ component and a slower Ca^{2+} component (Figs 1 and 2; Schiller *et al.* 1997; Schwindt & Crill, 1997), which can be isolated pharmacologically or by varying the time course of the input signal. Short-duration depolarizations may fail to activate the second component of the signal. If the duration of the input is long enough to activate the second component it can lead to the generation of a burst of axonal Na^+ APs. This suggests that the output pattern of APs is dependent on the nature of the input arriving at the tuft region. It should also be noted that the shorter the duration of the input, the higher the threshold for initiating the dendritic Na^+–Ca^{2+} AP.

Two components

The amplitude of the fast Na^+ component of the Na^+–Ca^{2+} AP as it propagates towards the soma remains relatively constant at distances > 300 μm from the soma. At shorter distances, the amplitude of the wavefront either increases, eventually reaching the size of the somatic AP, or it decreases and only an attenuated

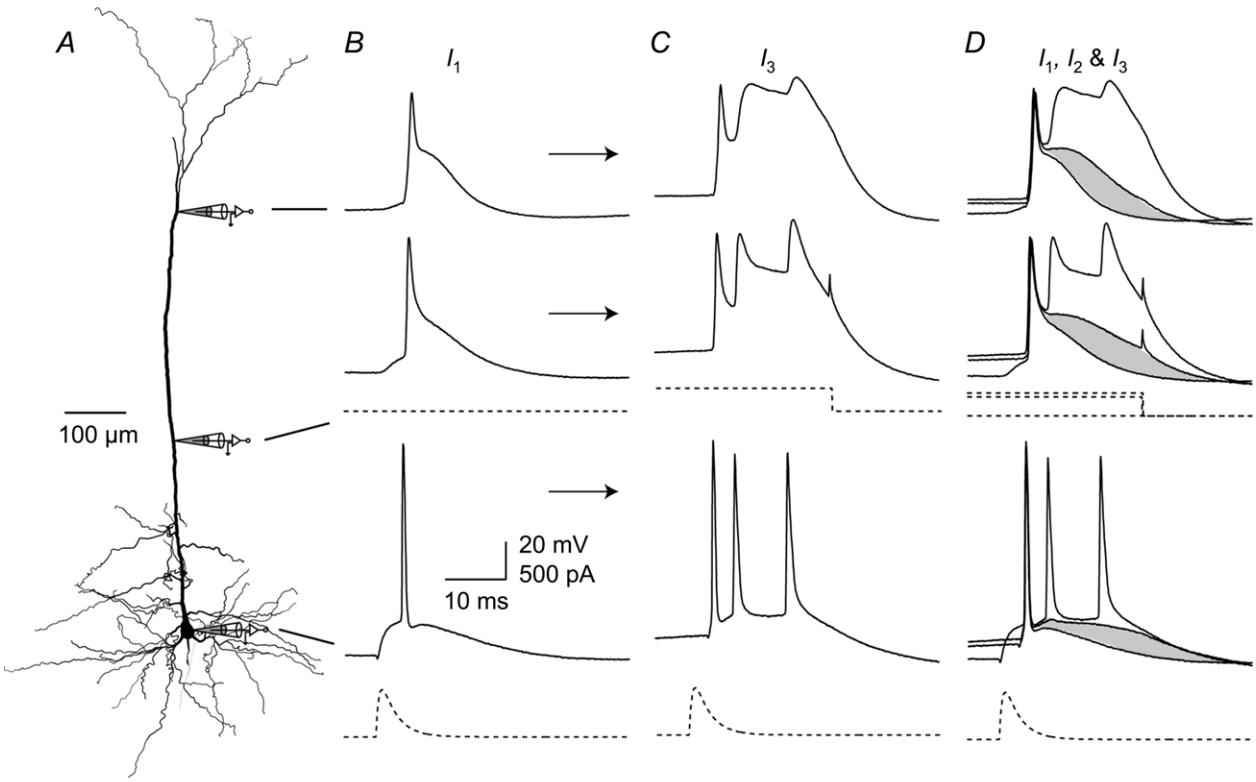

Figure 12. Dendritic depolarization controls the coupling of initiation zones

To test the relationship between bursting and dendritic depolarization, triple recordings were made with one distally located electrode, a proximally located electrode and a somatic electrode. *A*, reconstruction of a biocytin-filled L5 pyramidal neuron showing the locations of dendritic recordings (690 and 310 μm from the soma) and the recording at the soma. The three recordings shown in *B–D* represent different levels of depolarizing current injection (I_1, I_2 and I_3) at the proximal electrode, arranged vertically to correspond to the location of the electrodes. *B*, a single back-propagating AP was generated at the soma with an EPSP-shaped waveform (dashed trace at bottom). No current was injected at the proximal electrode (I_1). *C*, 500 pA current (I_3) injected at the proximal dendritic location starting 30 ms before the somatic current injection (current injection shown as dashed trace below middle recording trace) caused a burst of Na^+ APs at the soma and a long depolarizing potential in the dendrite. *D*, the traces from *B* and *C* are overlaid with the subthreshold current injection of 400 pA (I_2) showing the progressive activation of current in the dendrite. The shaded areas highlight the difference between the control and the trace just before threshold from which it can be seen that the increase is greatest in the proximal region.

potential is recorded at the soma like a 'boosted EPSP' (Schwindt & Crill, 1997). The dichotomy between amplification and attenuation begins in the proximal region of the apical dendrite (Fig. 15*A*). Dendritically evoked Na^+ APs propagating towards the soma in hippocampal neurons also appear to show variable propagation (Golding & Spruston, 1998).

Proximal dendritic influence on initiation zone coupling

Under *in vitro* conditions with intermediate duration current injection, there was an approximately equal fraction of neurons that had forward-propagating APs and failing APs. However, current injection at a proximal location on the apical dendrite has a large influence on propagation. APs can be caused to fail with hyperpolarization and the reverse with depolarization. The rising edge of the AP often has a point of inflection marking the onset of a second component. It is apparent at locations closer than ~500 μm from the soma, indicating that there is also regenerative activity in this zone. The fact that increasing depolarization leads to failure in this region might indicate the existence of a K^+ conductance which influences propagation as in CA1 pyramidal neurons (Hoffman *et al.* 1997). In some neurons, there are even two distinct peaks preceding the back-propagating Na^+ AP. The second peak emerges with depolarizing current applied to the proximal region and is unequivocal evidence for the generation of further regenerative activity in this region (Stuart *et al.* 1997). Thus, the proximal dendritic zone (from the soma to about 400 μm from the soma) forms a compartment in itself controlling the forward spread of distally initiated potentials. The apical oblique dendrites are situated in the appropriate location to have such an influence.

The proximal zone can have an additional influence on the generation of burst firing. Very small voltage deflections in this region can turn a single back-propagating Na^+ AP into a doublet or triplet. Recent work on hippocampal CA1 pyramidal neurons showed that the time constant for inactivation of dendritic Na^+ channels is much longer than that for dendritic A-type K^+ channels (37 *vs.* 6 ms with 20 mV depolarization above rest; Pan & Colbert, 2001). Thus, long depolarization of the dendrite alters the balance of Na^+ and K^+ conductances such that the dendrite becomes more excitable. For this to occur, however, the dendritic membrane fluctuation must take place in a time window that in our case was between ~10 and ~40 ms.

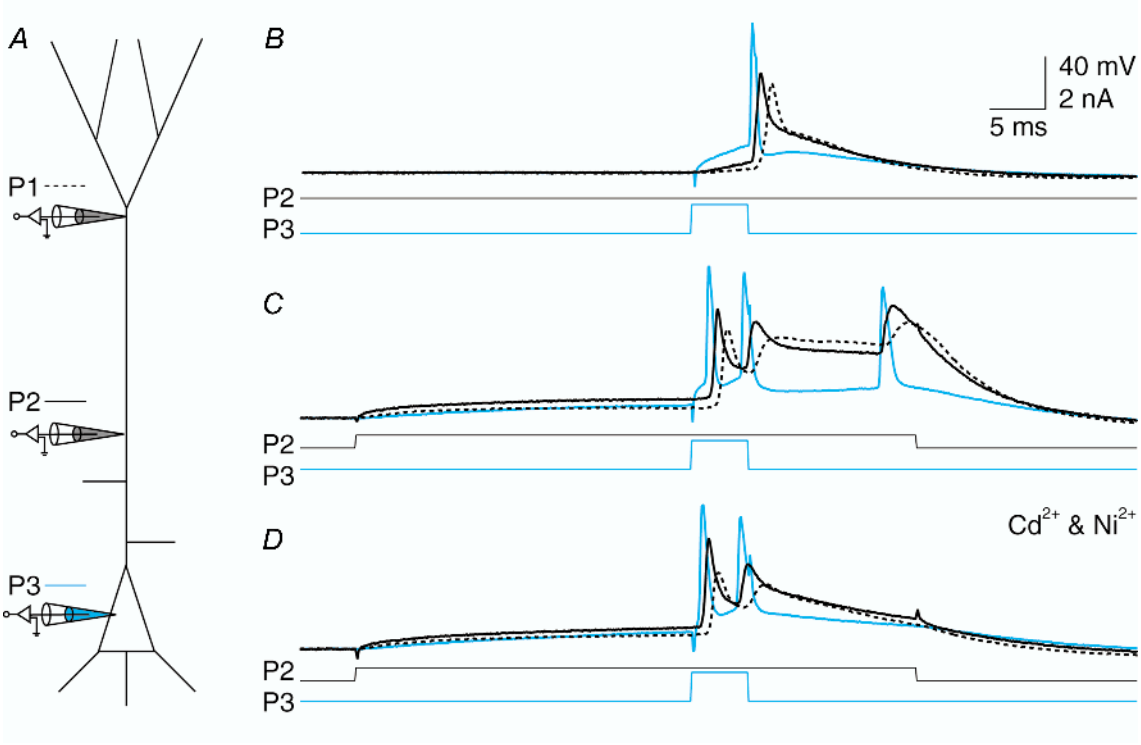

Figure 13. Dendritic Na^+–Ca^{2+} AP but not bursting is dependent on Ca^{2+}

A, schematic diagram showing the same experimental configuration as in Fig. 12. Here the electrodes were placed at 590 μm (P1, dashed line) and 280 μm (P2; black) from the soma and at the soma (P1; blue). *B*, an initial somatic Na^+ AP was elicited by current injection (1.1 nA) at the soma (current traces shown below). *C*, current injection at the proximal location (400 pA) caused the generation of a burst and a Na^+–Ca^{2+} AP at the dendritic location. *D*, application of 100 μM Ni^{2+} and 50 μM Cd^{2+} blocked the Na^+–Ca^{2+} AP and the third Na^+ AP in the burst but not the initial doublet, showing that the distal dendritic site was not responsible for the initial doublet.

Back propagation

A fast Na^+ AP generated in the axon (Stuart *et al.* 1997) is controlled by the proximal apical dendrite in a similar manner to forward-propagating potentials. The potential starts with the maximum amplitude at the axon and soma and decreases in amplitude along the apical dendrite. The recruitment of dendritic Na^+ channels depends on the amplitude of the back-propagating Na^+ AP at any point along the dendrite and the steady-state activation state of the channels, which is predominantly a function of the preceding Na^+ AP activity of the neuron. If the amplitude of the back-propagating Na^+ AP falls below the threshold for regenerative Na^+ channel activity, the Na^+ AP spreads passively after that point. The site at which this occurs is somewhere distal to the proximal dendritic zone ($> 300\ \mu m$ from the soma). This site of failure is very sensitive to the membrane potential in the proximal zone and can be altered by current injection in that region just as is the case with the forward-propagating AP. A dendritic Na^+–Ca^{2+} AP always leads to some depolarization at the soma. If the propagating dendritic potential increases towards the soma, the threshold for the initiation of a Na^+ AP in the axon is always reached. However, if the propagating dendritic potential decreases towards the soma, the threshold for initiating an axonal Na^+ AP can still be reached in some cases. The resulting back-propagating Na^+ AP then propagates to the dendritic initiation zone, which results in a Na^+–Ca^{2+} AP complex in that region.

Variability in amplitude *vs.* distance

The amplitudes of back-propagating APs become more variable at sites distal to the first segment of the apical

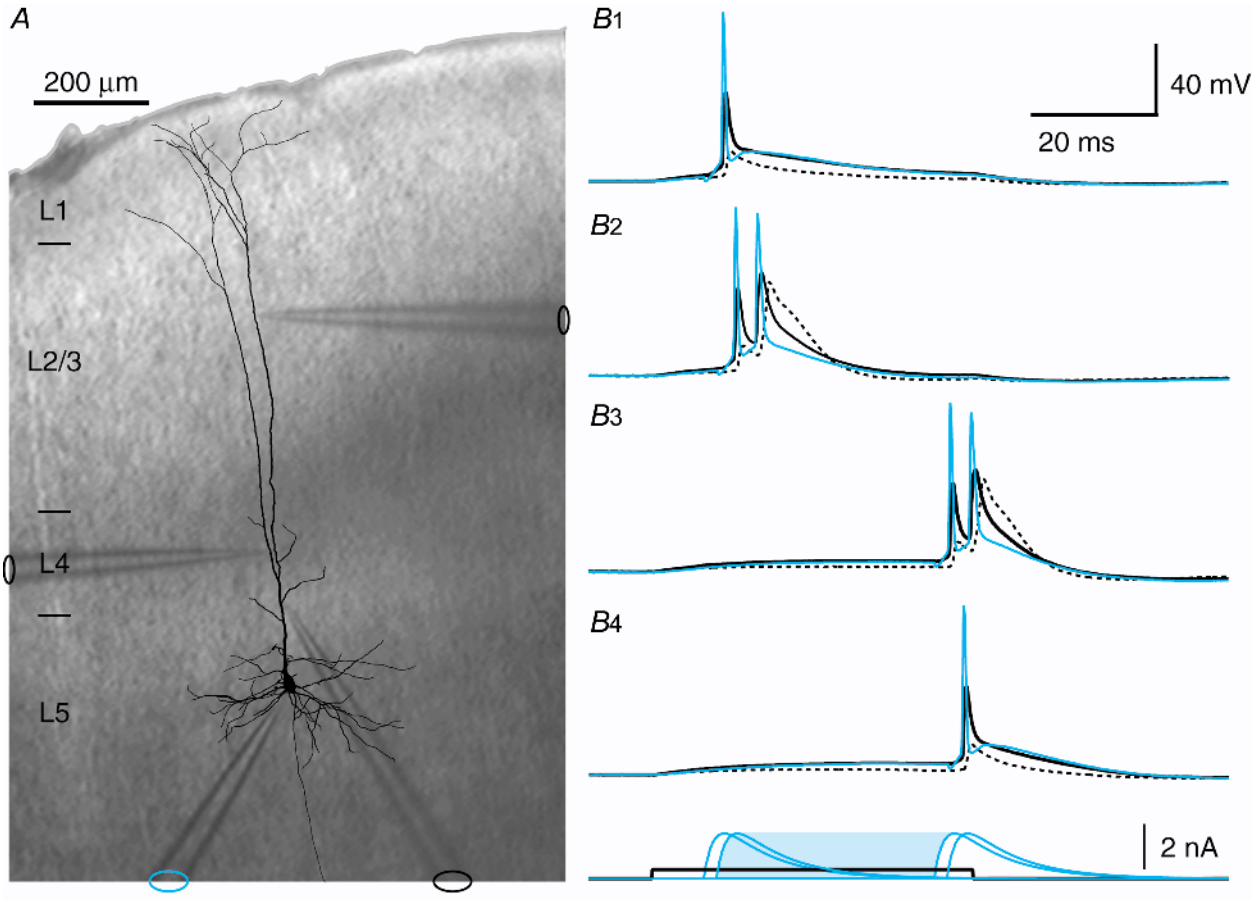

Figure 14. Timing of the combined input to the soma and proximal dendritic region

A, reconstruction of a biocytin-filled L5 neocortical pyramidal neuron overlaid on a photograph of the somatosensory cortex from a slice of rat brain during the experiment shown in *B*, with the silhouettes of the 4 electrodes indicating their positions. The layers of the cortex are indicated on the left-hand side. *B*1–4, current was injected at the electrode in layer 4 (electrode on the left, recording not shown) in the form of a 50 ms square pulse (0.4 nA) for each trace (1–4). Current injected at the somatic electrode (blue) with an EPSP waveform, which normally elicited a single Na^+ AP, elicited a doublet for the times indicated under *B*4 showing the current pulses (blue shaded time interval). This doublet caused a broadened potential after the second AP at the most proximal electrode (black) and especially at the distal electrode (dashed line).

dendrite (Fig. 15*A*, continuous lines). From simulations with compartmental models (Häusser *et al.* 1998; Rhodes, 1999; Vetter *et al.* 2001) it is predicted that in some cases the amplitude of the Na^+ AP can reach a constant value (and even increase somewhat) if it propagates to a point distal enough to be influenced by 'end-effects' of the dendrites. Furthermore, Na^+ APs are generated at a high frequency, the Na^+ channels that are more distal to the soma than ~500 μm inactivate (Jung *et al.* 1997) and the amplitude of the Na^+ AP is reduced (Fig. 15*A*, dashed line).

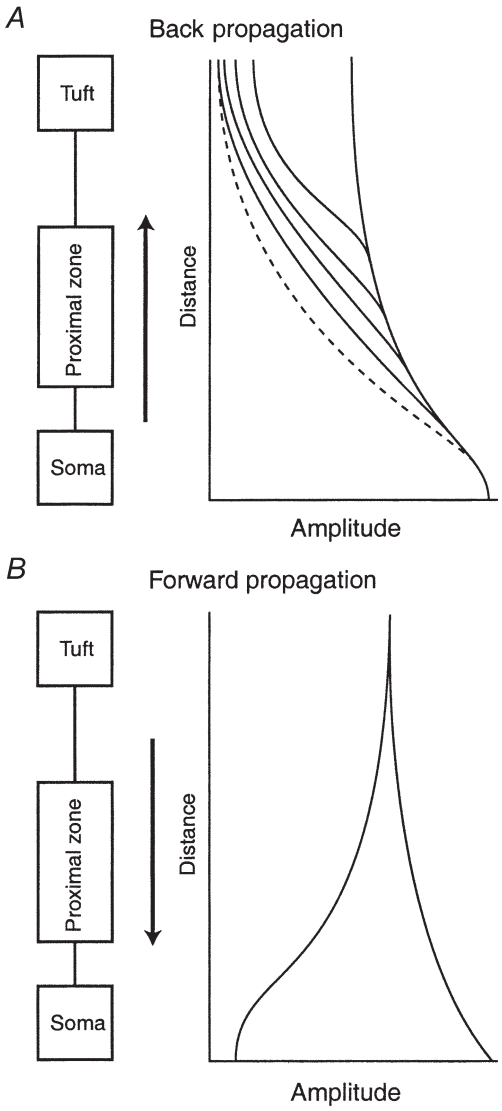

Figure 15. The propagation of regenerative potentials along the apical dendrite

A, the amplitude of Na^+ APs propagating from the soma back into the dendrites varies from cell to cell as a function of distance with increasing variability after the proximal apical zone (> 300 μm). The first AP in a train (continuous lines) sometimes maintained approximately the same amplitude from ~300 μm to well into the tuft. On the other hand, the subsequent APs in a train become progressively inactivated (dashed line) and failed to propagate fully to the tuft. *B*, dendritic Na^+–Ca^{2+} APs propagating towards the soma from the distal dendritic initiation zone fall into 2 categories: those that increase in amplitude until they reach the soma and those that fail somewhere in the proximal apical region and cause only a slight depolarization at the soma.

Presumably, under physiological conditions in which the pyramidal cell is generating APs, the amount of inactivation of distally located Na^+ channels varies and affects the extent of back propagation in a variable manner. Indeed *in vivo* recordings of dendritic behaviour appear to be characterized by variability between cells (Buzsáki & Kandel, 1998; Kamondi *et al.* 1998; Helmchen *et al.* 1999). In addition, the morphology of the dendritic arbor and passive properties as well as the distribution of voltage-gated channels will both influence AP propagation (Schaefer *et al.* 2000). Cells with thicker apical dendrites are likely to be more favourable for propagation (London *et al.* 1999). There are also factors that might specifically affect the *in vivo* situation such as background synaptic activity, spontaneous inhibitory inputs and neuromodulatory effects (Colmers & Bleakman, 1994; Kim *et al.* 1995; Larkum *et al.* 1999*b*; Paré *et al.* 1998*a*,*b*; Zhu & Heggelund, 2001). In the *in vitro* conditions of this study, it appears that the morphology and channel distribution in pyramidal cells are such that AP propagation can be influenced by small changes in membrane potential in the dendritic arbor.

Since the measured amplitude of the back-propagating Na^+ AP is also sensitive to the access resistance across the electrode tip, there is the possibility of experimental error contributing to the variability in AP amplitudes. This error would be expected to increase as a function of distance too, due to the decreasing width of the apical dendrite. It is unlikely that this was the major cause of variation because we could control the size of the AP in the distal dendrite by current injection into the proximal dendrite. This was direct proof that the distal electrodes could record large events. Recordings where the access resistance became too large (> ~70 MΩ) were not used for the measurement of AP amplitude.

Mechanisms for amplification of back-propagating action potentials

Only the fast initial component of the forward-propagating AP is modulated by dendritic current injection. This component is very similar in duration to the back-propagating AP and the mechanisms are probably the same in the two cases. There are Na^+ and K^+ channels in the apical dendrites of L5 neocortical pyramidal neurons (Stuart & Sakmann, 1994; Bekkers, 2000; Korngreen & Sakmann, 2000), which undoubtedly affect the amplitude and propagation of suprathreshold potentials. The back-propagating AP has been shown to be enhanced by dendritically originating EPSPs in both L5 neocortical and CA1 pyramidal neurons (Magee & Johnston, 1997; Stuart & Häusser, 1999). In the former case this was attributed to activation of Na^+ channels. In the case of CA1 pyramidal neurons it has been suggested that the modulation in amplitude of the back-

propagating APs arises from the properties of fast K^+ channels (Hoffman *et al.* 1997). Since both classes of channel exist in the dendrites of L5 pyramidal neurons in approximately equal densities and are both affected by fluctuations in V_m around resting potential, it is likely that both channels contribute to the changes seen in dendritic AP amplitude as a result of dendritic current injections.

Three-compartment model of a thick-tufted pyramidal neuron

The experimental results are best explained by a model of L5 neocortical pyramidal neurons with three functional compartments. The distal apical initiation zone and the somato-basal-axonal regions have been proposed as two functional compartments (Yuste *et al.* 1994; Schiller *et al.* 1997). The data reported here indicate that the oblique dendrites situated in the proximal apical zone constitute a third compartment (Fig. 16*A*). It is obvious that each of the three functional zones (dashed boxes) corresponds to an anatomically distinguishable region of the dendritic arborization; the distal tuft (compartment A), the oblique dendrites (compartment B) and the basal dendrites (compartment C). Inputs arriving at these three dendritic domains will have a specific influence on both the initiation and the propagation of potentials in the pyramidal neuron over and above their influence on the ongoing integration occurring at the axon initial segment. The tuft and basal compartments control the initiation of APs although the proximal apical dendritic zone may also initiate APs under some circumstances (Fig. 4 and Turner *et al.* 1991; Regehr *et al.* 1993; Schwindt & Crill, 1997; Stuart *et al.* 1997; Golding & Spruston, 1998). The proximal dendritic region can be thought of functionally

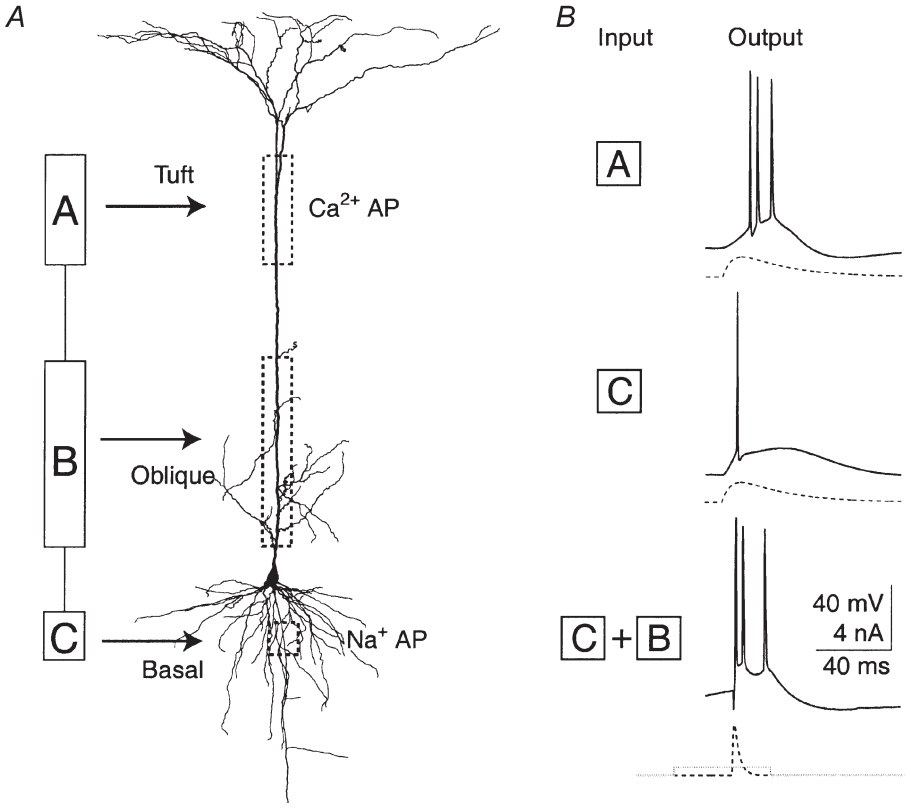

Figure 16. Simplified representation of a L5 neocortical pyramidal neuron and the relationship between input location and AP pattern

A, representation of a L5 neocortical pyramidal neuron with 3 functional compartments compared to the morphology of a reconstructed biocytin-filled L5 pyramidal neuron from the somatosensory cortex. Compartment A corresponds to the distal apical initiation zone and the tuft dendrites. Compartment B corresponds to the axonal initiation zone and the basal dendrites. Compartment C corresponds to the proximal apical dendrite and oblique dendrites. *B*, input to the distal dendrite tends to cause a burst of Na^+ APs whereas the same input to the soma tends to cause single APs or regularly spaced spikes. Typical examples are shown here of the response of the same neuron to a 10 ms time to peak EPSP waveform (dashed traces) injected in either compartment A or compartment C at threshold current levels. Input to compartment B tends to improve the coupling between compartments A and C. After priming the proximal dendritic compartment (B) with a small current injection, a short EPSP waveform (time to peak of 3 ms) at the soma leads to a burst of Na^+ APs (bottom traces).

as a 'coupling zone' that controls the propagation of dendritic regenerative potentials in both directions and thereby controls the coupling of the other two AP initiation zones.

Function of L5 pyramids

The three compartments of L5 pyramids are located in the cortex such that input from higher cortical areas ('feedback') arrives predominantly at the tuft compartment (compartment A), whereas direct sensory input and intra-columnal input ('feedforward') arrives at the proximal and basal compartments (compartments B and C; Cauller, 1995). We propose that this arrangement of functional and anatomical compartments of innervation ensures the dominance of higher cortical feedback inputs when they coincide with ongoing columnar activity. There are a few indications that models of networks consisting of elements with correlates for active dendrites and with two initiation zones are improved with respect to storage and retrieval of information (Horn *et al.* 1999; Levy *et al.* 1999; Koerding & Koenig, 2000; Siegel *et al.* 2000). These networks work best when 'far away' cortical areas are connected to a 'dendritic' compartment which summates non-linearly, whereas input from 'nearby' areas is connected to a 'somatic' compartment which summates linearly.

Functional consequences of different input distributions

The functional three-compartment description of L5 pyramidal neurons was derived from two convergent lines of evidence. The first is based on the dendritic arborization, which has three distinct regions, defining classes of synaptic input into the cell. The second is based on the electrical response of cells to current injected into the apical dendrite or soma near these three regions. The type of regenerative potential elicited and the degree of interaction between the zones is dependent on not only the location but also the time course of input. The response of L5 neurons to common types of input based on the location and duration of the synaptic input would be consistent with the following simple rules for input–output relations of L5 pyramidal neurons *in vitro* (Fig. 16*B*). (1) Input to basal and proximal apical dendritic regions generates short Na^+ APs with a pattern of single or evenly spaced APs. (2) Input to the distal tuft region generates long Na^+–Ca^{2+} APs that cause bursts of unevenly spaced APs. (3) Input to the proximal dendritic region couples or decouples the two AP initiation zones, which determines whether the activation of one initiation zone leads to the activation of the other. (4) The basal dendritic region defines the dominant type of output under conditions of weak coupling between the initiation zones and the distal region dominates when the coupling is tight.

In addition to these simple rules, the duration and timing of inputs to the different regions dictate the precise AP firing pattern in a more complex manner. We have explored some of the rules here and elsewhere based on likely physiological combinations (Larkum *et al.* 1999*a*,*b*), but an exhaustive study of all the combinations has yet to be done and is perhaps best suited to modelling studies.

Conclusion

The two action potential initiation zones in the distal dendrite and axon of L5 pyramidal neurons interact to generate a variety of AP patterns. The degree of interaction is controlled by the membrane potential along the proximal apical dendrite. Thus the most parsimonious description of the L5 pyramidal neuron that accounts for its firing properties includes three compartments. The three compartments extending over the different cortical layers facilitate the separation into classes of inputs based on their laminar position in the cortex. In this way, the electrical activity of the main output neurons of the cortex reflects the laminal distribution of synaptic activity within a given cortical column.

Bekkers, J. M. (2000). Properties of voltage-gated potassium currents in nucleated patches from large layer 5 cortical pyramidal neurons of the rat. *Journal of Physiology* **525**, 593–609.

Buzsáki, G. & Kandel, A. (1998). Somadendritic backpropagation of action potentials in cortical pyramidal cells of the awake rat. *Journal of Neurophysiology* **79**, 1587–1591.

Buzsáki, G., Penttonen, M., Nádasdy, Z. & Bragin, A. (1996). Pattern and inhibition-dependent invasion of pyramidal cell dendrites by fast spikes in the hippocampus in vivo. *Proceedings of the National Academy of Sciences of the USA* **93**, 9921–9925.

Cauller, L. (1995). Layer I of primary sensory neocortex: where top-down converges upon bottom-up. *Behavioural Brain Research* **71**, 163–170.

Colmers, W. F. & Bleakman, D. (1994). Effects of neuropeptide Y on the electrical properties of neurons. *Trends in Neurosciences* **17**, 373–379.

Denk, W., Delaney, K. R., Gelperin, A., Kleinfeld, D., Strowbridge, B. W., Tank, D. W. & Yuste, R. (1994). Anatomical and functional imaging of neurons using 2-photon laser scanning microscopy. *Journal of Neuroscience Methods* **54**, 151–162.

Golding, N. L. & Spruston, N. (1998). Dendritic sodium spikes are variable triggers of axonal action potentials in hippocampal CA1 pyramidal neurons. *Neuron* **21**, 1189–1200.

Häusser, M., Vetter, P. & Roth, A. (1998). Action-potential backpropagation depends on dendritic geometry. *Society for Neuroscience Abstracts* **24**, 1813.

Helmchen, F., Svoboda, K., Denk, W. & Tank, D. W. (1999). In vivo dendritic calcium dynamics in deep-layer cortical pyramidal neurons. *Nature Neuroscience* **2**, 989–996.

Hoffman, D. A., Magee, J. C., Colbert, C. M. & Johnston, D. (1997). K^+ channel regulation of signal propagation in dendrites of hippocampal pyramidal neurons. *Nature* **387**, 869–875.

Horn, D., Levy, N. & Ruppin, E. (1999). The importance of nonlinear dendritic processing in multimodular memory networks. *Neurocomputing* **26-7**, 389–394.

Johnston, D., Magee, J. C., Colbert, C. M. & Cristie, B. R. (1996). Active properties of neuronal dendrites. *Annual Review of Neuroscience* **19**, 165–186.

Jung, H. Y., Mickus, T. & Spruston, N. (1997). Prolonged sodium channel inactivation contributes to dendritic action potential attenuation in hippocampal pyramidal neurons. *Journal of Neuroscience* **17**, 6639–6646.

Kamondi, A., Acsády, L. & Buzsáki, G. (1998). Dendritic spikes are enhanced by cooperative network activity in the intact hippocampus. *Journal of Neuroscience* **18**, 3919–3928.

Kim, H. G., Beierlein, M. & Connors, B. W. (1995). Inhibitory control of excitable dendrites in neocortex. *Journal of Neurophysiology* **74**, 1810–1814.

Koerding, K. P. & Koenig, P. (2000). Learning with two sites of synaptic integration. *Network* **11**, 25–39.

Korngreen, A. & Sakmann, B. (2000). Voltage-gated K^+ channels in layer 5 neocortical pyramidal neurones from young rats: subtypes and gradients. *Journal of Physiology* **525**, 621–639.

Larkum, M. E., Kaiser, K. M. & Sakmann, B. (1999*a*). Calcium electrogenesis in distal apical dendrites of layer 5 pyramidal cells at a critical frequency of back-propagating action potentials. *Proceedings of the National Academy of Sciences of the USA* **96**, 14600–14604.

Larkum, M. E., Zhu, J. J. & Sakmann, B. (1999*b*). A new cellular mechanism for coupling inputs arriving at different cortical layers. *Nature* **398**, 338–341.

Levy, N., Horn, D. & Ruppin, E. (1999). Associative memory in a multimodular network. *Neural Computation* **11**, 1717–1737.

London, M., Meunier, C. & Segev, I. (1999). Signal transfer in passive dendrites with nonuniform membrane conductance. *Journal of Neuroscience* **19**, 8219–8233.

Magee, J. C. & Johnston, D. (1997). A synaptically controlled, associative signal for Hebbian plasticity in hippocampal neurons. *Science* **275**, 209–213.

Mainen, Z. F. & Sejnowski, T. J. (1996). Influence of dendritic structure on firing pattern in model neocortical neurons. *Nature* **382**, 363–366.

Mel, B. W. (1993). Synaptic integration in an excitable dendritic tree. *Journal of Neurophysiology* **70**, 1086–1101.

Pan, E. & Colbert, C. M (2001). Subthreshold inactivation of Na^+ and K^+ channels supports activity-dependent enhancement of back-propagating action potentials in hippocampal CA1. *Journal of Neurophysiology* **85**, 1013–1016.

Paré, D., Lang, E. J. & Destexhe, A. (1998*a*). Inhibitory control of somatodendritic interactions underlying action potentials in neocortical pyramidal neurons *in vivo*: an intracellular and computational study. *Neuroscience* **84**, 377–402.

Paré, D., Shink, E., Gaudreau, H., Destexhe, A. & Lang, E. J. (1998*b*). Impact of spontaneous synaptic activity on the resting properties of cat neocortical pyramidal neurons *in vivo*. *Journal of Neurophysiology* **79**, 1450–1460.

Pinsky, P. F. & Rinzel, J. (1994). Intrinsic and network rhythmogenesis in a reduced Traub model for CA3 neurons. *Journal of Computational Neuroscience* **1**, 39–60.

Pockberger, H. (1991). Electrophysiological and morphological properties of rat motor cortex neurons *in vivo*. *Brain Research* **539**, 181–190.

Regehr, W., Kehoe, J. S., Ascher, P. & Armstrong, C. (1993). Synaptically triggered action potentials in dendrites. *Neuron* **11**, 145–151.

Reuveni, I., Friedman, A., Amitai, Y. & Gutnick, M. J. (1993). Stepwise repolarization from Ca^{2+} plateaus in neocortical pyramidal cells: evidence for nonhomogeneous distribution of HVA Ca^{2+} channels in dendrites. *Journal of Neuroscience* **13**, 4609–4621.

Rhodes, P. A. (1999). Functional implications of active currents in the dendrites of pyramidal neurons. In *Cerebral Cortex*, vol. 13, ed. Ulinski, P. & Jones, E. G., pp. 139–200. Plenum Press, New York.

Schaefer, A. T., Roth, A. & Sakmann, B. (2000). Morphological correlates of BAC-firing threshold in model layer 5 pyramidal neurons. *European Journal of Neuroscience* **12**, 369.

Schiller, J., Major, G., Koester, H. J. & Schiller, Y. (2000). NMDA spikes in basal dendrites of cortical pyramidal neurons. *Nature* **404**, 285–289.

Schiller, J., Schiller, Y., Stuart, G. & Sakmann, B. (1997). Calcium action potentials restricted to distal apical dendrites of rat neocortical pyramidal neurons. *Journal of Physiology* **505**, 605–616.

Schwindt, P. & Crill, W. (1999). Mechanisms underlying burst and regular spiking evoked by dendritic depolarization in layer 5 cortical pyramidal neurons. *Journal of Neurophysiology* **81**, 1341–1354.

Schwindt, P. C. & Crill, W. E. (1997). Local and propagated dendritic action potentials evoked by glutamate iontophoresis on rat neocortical pyramidal neurons. *Journal of Neurophysiology* **77**, 2466–2483.

Siegel, M., Körding, K. P. & König, P. (2000). Integrating top-down and bottom-up sensory processing by somato-dendritic interactions. *Journal of Computational Neuroscience* **8**, 161–173.

Spencer, W. A. & Kandel, E. R. (1960). Electrophysiology of hippocampal neurons. *Journal of Neurophysiology* **24**, 272–285.

Spruston, N., Schiller, Y., Stuart, G. & Sakmann, B. (1995). Activity dependent action potential invasion and calcium influx into hippocampal CA1 dendrites. *Science* **268**, 297–300.

Stuart, G., Schiller, J. & Sakmann, B. (1997). Action potential initiation and propagation in rat neocortical pyramidal neurons. *Journal of Physiology* **505**, 617–632.

Stuart, G. J., Dodt, H. U. & Sakmann, B. (1993). Patch-clamp recordings from the soma and dendrites of neurons in brain slices using infrared video microscopy. *Pflügers Archiv* **423**, 511–518.

Stuart, G. J. & Häusser, M. (1999). Amplification of backpropagating action potentials by EPSPs. *Society for Neuroscience Abstracts* **25**, 1739.

Stuart, G. J. & Sakmann, B. (1994). Active propagation of somatic action potentials into neocortical pyramidal cell dendrites. *Nature* **367**, 69–72.

Turner, R. W., Meyers, D. E., Richardson, T. L. & Barker, J. L. (1991). The site for initiation of action potential discharge over the somatodendritic axis of rat hippocampal CA1 pyramidal neurons. *Journal of Neuroscience* **11**, 2270–2280.

Vetter, P., Roth, A. & Häusser, M. (2001). Propagation of action potentials in dendrites depends on dendritic morphology. *Journal of Neurophysiology* **85**, 926–937.

Williams, S. R. & Stuart, G. J. (1999). Mechanisms and consequences of action potential burst firing in rat neocortical pyramidal neurons. *Journal of Physiology* **521**, 467–482.

Wong, R. K. & Stewart, M. (1992). Different firing patterns generated in dendrites and somata of CA1 pyramidal neurones in guinea-pig hippocampus. *Journal of Physiology* **457**, 675–687.

Yuste, R., Gutnick, M. J., Saar, D., Delaney, K. R. & Tank, D. W. (1994). Ca^{2+} accumulations in dendrites of neocortical pyramidal neurons: an apical band and evidence for two functional compartments. *Neuron* **13**, 23–43.

Zhu, J. J. (2000). Maturation of layer 5 neocortical pyramidal neurons: amplifying salient layer 1 and layer 4 inputs by Ca^{2+} action potentials in adult rat tuft dendrites. *Journal of Physiology* **526**, 571–587.

Zhu, J. J. & Connors, B. W. (1999). Intrinsic firing patterns and whisker-evoked synaptic responses of neurons in the rat barrel cortex. *Journal of Neurophysiology* **81**, 1171–1183.

Zhu, J. J. & Heggelund, P. (2001). Muscarinic regulation of axonal and dendritic outputs of rat thalamic interneurons: a new cellular mechanism for uncoupling distal dendrites. *Journal of Neuroscience* **21**, 1148–1159.

Acknowledgements

M.E.L. and J.J.Z. were supported by postdoctoral fellowships from the Max-Planck Society.

Corresponding author

M. E. Larkum: Max-Planck-Institut für medizinische Forschung, Abteilung Zellphysiologie, Jahnstraße 29, D-69120 Heidelberg, Germany.

Author's present address

J. J. Zhu: Cold Spring Harbor Laboratory, Jones 1 Bungtown Road, Cold Spring Harbor, NY 11724, USA.